Xie *et al. Energy Mater.* **2025**, *5*, 500025
DOI: 10.20517/energymater.2024.183

Energy Materials

Article

Open Access

Regulating the solvation environment of hybrid electrolytes towards high-temperature zinc-ion storage

Yulin Xie, Qingyun Dou*, Guosheng Li, Yuecong Chen, Xingbin Yan*

School of Materials Science and Engineering, Sun Yat-sen University, Guangzhou 510006, Guangdong, China.

***Correspondence to:** Dr. Qingyun Dou and Dr. Xingbin Yan, School of Materials Science and Engineering, Sun Yat-sen University, No. 132, Waihuan Dong Road, Higher Education Mega Center, Guangzhou 510006, Guangdong, China. E-mail: douqy3@mail.sysu.edu.cn; yanxb3@mail.sysu.edu.cn

How to cite this article: Xie, Y.; Dou, Q.; Li, G.; Chen, Y.; Yan, X. Regulating the solvation environment of hybrid electrolytes towards high-temperature zinc-ion storage. *Energy Mater.* **2025**, *5*, 500025. https://dx.doi.org/10.20517/energymater.2024.183

Received: 23 Sep 2024 **First Decision:** 6 Nov 2024 **Revised:** 30 Nov 2024 **Accepted:** 10 Dec 2024 **Published:** 16 Jan 2025

Academic Editor: Jiazhao Wang **Copy Editor:** Ping Zhang **Production Editor:** Ping Zhang

Abstract

Zinc-ion batteries (ZIBs) are being explored as a potential alternative to lithium-ion batteries owing to the growing demand for safer, more sustainable, cost-effective energy storage technologies. In such systems, electrolytes, as one of the key components, have a decisive impact on their electrochemical performance. However, Zn anodes in traditional aqueous electrolytes exhibit drawbacks such as severe hydrogen evolution reactions, Zn corrosion and passivation especially at high temperatures, leading to poor cycling performance of ZIBs. Herein, we designed and evaluated a series of hybrid electrolytes consisting of zinc tetrafluoroborate hydrate [$Zn(BF_4)_2{\cdot}xH_2O$] as the solute and various organic solvents [tetraglyme (G4), propylene carbonate, and dimethylformamide] for high-temperature ZIBs. Comparative analysis revealed that G4-based hybrid electrolytes exhibit a unique Zn^{2+} solvation structure primarily surrounded by organic solvent rather than H_2O, which substantially reduces H_2O-related side reactions and thus promotes more reversible Zn deposition than propylene carbonate-based and dimethylformamide-based hybrid electrolytes. The superiority of G4-based hybrid electrolyte is further confirmed by long stable cycling life of the corresponding Zn||Zn symmetric cell (> 350 h) and Zn-ion capacitor full cell (over 1,400 cycles with 90.7% capacity retention) at 60 °C.

Keywords: Hybrid electrolyte, solvation structure, high temperature, zinc anode

INTRODUCTION

Zinc-ion batteries (ZIBs) are emerging as a promising alternative to lithium-ion batteries, driven by the growing demand for safer and more sustainable energy storage technologies[1-4]. A typical ZIB consists of a Zn anode, a Zn^{2+} storage material as the cathode, and an electrolyte[5-7]. Zn anodes offer key advantages such as high abundance (100 times that of lithium), low redox potential (-0.76 V *vs.* standard hydrogen electrode), compatibility with water, and high theoretical capacity (820 mAh g^{-1})[8-10]. However, several challenges hinder their widespread applications[11,12]. A primary issue is the corrosion and side reactions in aqueous electrolytes, which damage the electrode, compromising both stability and cycling life[13,14]. Additionally, uneven Zn deposition and dendrite growth during charging can cause short circuits and battery failure[15-17]. Despite these challenges, Zn anodes remain a strong candidate for Zn-based energy storage technologies[18,19].

Ongoing research is addressing the above issues, focusing on developing advanced electrolytes that critically influence the overall performance of Zn anodes[20-22]. Although traditional aqueous electrolytes provide high ionic conductivity and safety, they present significant challenges such as a narrow electrochemical stability window, vulnerability to water splitting, and thermal instability, all of which degrade battery performance, particularly at elevated temperatures[23,24]. To promote the practical applications of ZIBs in high-temperature environments, it is essential to develop alternative electrolytes that can overcome these limitations[25-27]. Electrolyte research for ZIBs has largely focused on enhancing cycling life and rate capability of Zn anodes, while less attention has been paid to temperature adaptability[28-31]. Currently, strategies to improve temperature adaptability include increasing electrolyte concentration and incorporating electrolyte additives[32,33]. For example, Zhang *et al.* have noted that a highly-concentrated 3 M zinc trifluoromethylsulfonate [$Zn(OTf)_2$] electrolyte supports better cyclic stability than the diluted one [e.g., 1 M $Zn(OTf)_2$][34]. This concentrated electrolyte works well in rough conditions at both low (-10 °C) and high (50 °C) temperatures, because the high-concentration electrolyte effectively reduces the water activity and related side reactions. Wang *et al.* have demonstrated that ethylene glycol (EG) as a water blocker promotes the formation of a localized high-concentration electrolyte for stable and dendrite-free cycling of the Zn anode[35]. Even at a high temperature of 60 °C, the cell successfully operates for 900 cycles. The above approaches expand the applicable temperature range of aqueous electrolytes; however, the high water content in these electrolytes would cause undesired side reactions and the Zn dendrite formation[36]. As a result, the high-temperature stability of ZIBs remains a challenge that has yet to be fully addressed[37,38].

In this study, an ether-based hybrid electrolyte with extremely low water content is designed using tetraglyme (G4) as the solvent and zinc tetrafluoroborate hydrate [$Zn(BF_4)_2{\cdot}xH_2O$] as the solute for high-temperature ZIBs. The superiority of G4-based electrolyte is revealed by systematically comparing with the other two hybrid electrolytes using propylene carbonate (PC) and dimethylformamide (DMF) organic solvents-with $Zn(BF_4)_2{\cdot}xH_2O$ as the solute. Theoretical calculations and experimental results demonstrate that G4 strongly coordinates with Zn^{2+} ions, substantially reducing the amount of H_2O in the Zn^{2+} solvation sheath. This unique Zn^{2+} solvation structure effectively suppresses the hydrogen evolution reaction (HER) and dendrite formation. The optimal G4-based hybrid electrolyte shows remarkable high-temperature stability, enabling Zn||Zn symmetrical cell to operate for > 350 h at 60 °C. Additionally, when tested in a Zn-ion capacitor with an activated carbon (AC) cathode, the hybrid electrolyte allows the cell to retain 90% of its initial capacity after 1,400 cycles at 60 °C. These results highlight the effectiveness of G4-based hybrid electrolytes in enhancing the high-temperature performance of ZIBs, paving the way for their use in applications that require reliable energy storage under extreme conditions.

EXPERIMENTAL SECTION

Preparation of hybrid electrolyte

The purchased $Zn(BF_4)_2{\cdot}xH_2O$ (Macklin), DMF (> 99%, Macklin), PC (99%, Aladdin), G4 (99%, Aladdin), diethyl carbonate (DEC, 99%, Macklin), and dimethyl sulfoxide (DMSO, 99%, Macklin) were used without further purification. $Zn(BF_4)_2{\cdot}xH_2O$ solutions with specific proportions of organic solvents were prepared as electrolyte samples.

Preparation of electrodes and cells

A commercial Zn plate (150 μm in thickness) was cut into a circle (diameter 10mm) and directly served as the electrode of Zn||Zn symmetric cell and Zn||AC full cell. Commercial AC (YP-50F) was used as the cathode material of Zn||AC full cell. To prepare the AC electrode, the AC powder, acetylene black, and binder [poly(tetrafluoroethylene), PTFE] were mixed in a weight ratio of 8:1:1 to form a homogeneous slurry by adding moderate water and ethanol; the slurry was then coated on stainless steel mesh. The AC electrode dried at 120 °C for 12h. Its mass loading was ~1 mg cm^{-1}. The as-prepared solution and glass fiber (GF/D, Whatman) were used as the electrolyte and separator, respectively.

Materials characterization

The morphologies of Zn foils were investigated by a the Lehn Institute of Functional Materials (LIFM-Ultra-high resolution field emission scanning electron microscope (SEM, SU8010), with energy dispersive X-ray spectroscopy (EDS) for the element determination. The surface components of electrodes were characterized on an X-ray photoelectron spectrometer (XPS, Nexsa) with a monochromatic Al-Kα source (Mono AlKα, 1486.6eV, 12kV 720W). X-ray diffraction (XRD) patterns were collected on an X-ray diffractometer (D-MAX 2200 VPC, RIGAKU). Fourier transform infrared (FTIR) spectra of the electrolytes were recorded using a LIFM FTIR instrument. The ionic conductivities of electrolytes were measured using a Conductivity Meter (DDS 11A, Shanghai Youke). The adiabatic calorimeter experiments in the "heat-wait-seek mode" were recorded for the electrolytes using an accelerating rate calorimeter (ARC, Thermal Hazard Technology). The "heat-wait-seek mode" works as follows: the sample in the adiabatic calorimeter was heated from room temperature to 250 °C in a gradient of 5 °C, and at each temperature the sample was kept for five minutes to monitor any thermal responses.

Electrochemical measurements

The cyclic voltammetry (CV), chronoamperometry (CA), linear sweep voltammetry (LSV), and electrochemical impedance spectroscopy (EIS) measurements were conducted using an electrochemical workstation (CHI660E, Shanghai, China). The Nyquist plots were obtained using EIS with a frequency range from 100 kHz to 0.1 Hz and a potential amplitude of 10 mV. The galvanostatic charge/discharge (GCD) measurements were conducted using the Neware Battery Measurement System (CT-ZWJ-4'S-T-1U, Shenzhen, China).

RESULTS AND DISCUSSION

Performance characterization of symmetric cells with hybrid electrolytes

We prepared hybrid electrolytes using $Zn(BF_4)_2{\cdot}xH_2O$ as the solute[39,40] and various representative organic solvents of high dielectric constants: PC, DMF, G4, DEC, and DMSO. As shown in Supplementary Figure 1, $Zn(BF_4)_2{\cdot}xH_2O$ can be fully dissolved in PC, DMF and G4 to achieve a concentration of 0.5 M, while 0.5 M $Zn(BF_4)_2{\cdot}xH_2O$ in DEC and DMSO were not clear solutions. Moreover, acetonitrile (AN) was not considered as a solvent due to its low boiling point (81.6 °C). Therefore, the PC-, DMF-, and G4-based hybrid electrolytes were evaluated in Zn||Zn symmetric cells at 30 °C and 60 °C. The plating/stripping tests were conducted at a current density of 1 mA cm^{-2} and a capacity of 0.5 mAh cm^{-2}. As illustrated in Figure 1A and B, the cells using G4-based electrolytes demonstrated the most stable cycling performance,

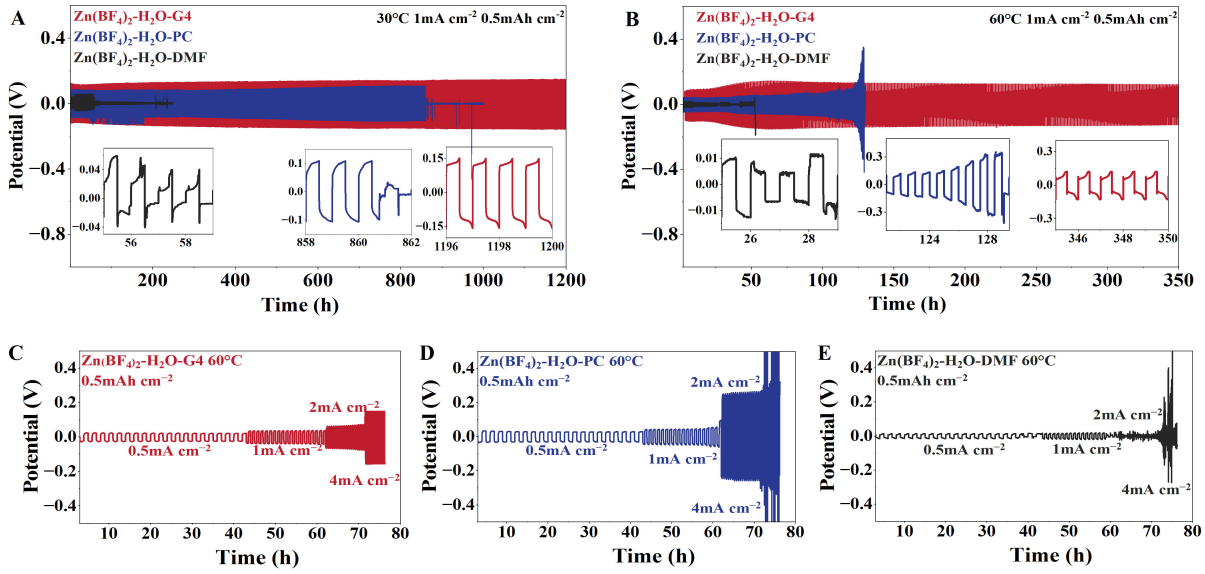

Figure 1. Cycling performance of the Zn||Zn symmetric cells using three hybrid electrolytes. Galvanostatic Zn plating/stripping under 1mA cm^{-2} and 0.5 mAh cm^{-2} at (A) 30 °C and (B) 60 °C; Galvanostatic Zn plating/stripping under different current densities and 0.5 mAh cm^{-2} capacity in (C) G4-based; (D) PC-based; and (E) DMF-based hybrid electrolytes at 60 °C. PC: Propylene carbonate; DMF: Dimethylformamide.

followed by those using PC-based electrolytes, while the cells using DMF-based electrolytes showed the poorest cycling stability. Specifically, at 30 °C [Figure 1A], the cell using a G4-based electrolyte cycled stably for over 1,200 h, while that using PC-based electrolyte experienced an evident decrease in polarization potential after ~860 h attributed to a short circuit. In sharp contrast, the cell using DMF-based electrolyte showed a drop in polarization potential solely after ~55 h. At 60 °C [Figure 1B], the cell using G4-based electrolyte maintained stable cycling for more than 350 h. In comparison, the cells using PC- and DMF-based hybrid electrolytes exhibited a substantial increase and fluctuation in polarization potential after ~120 h and ~20 h, respectively, indicating cell failure. Given the superiority of Zn||Zn symmetric cell in G4-based electrolyte, its cycling stabilities at higher temperatures were tested [Supplementary Figure 2]. At 80 °C, the cell could cycle stably for 90 h at 0.5 mA cm^{-2} and 0.25 mAh cm^{-2}. With temperature increased to 100 °C, the cell failed rapidly after ten hours. We further assessed cell stability at different current densities at 60 °C [Figure 1C-E]. The cell using G4-based electrolyte maintained stable cycling across varying current densities without significant changes in polarization potential [Figure 1C]. In contrast, the cells using PC-based and DMF-based electrolytes showed marked fluctuations in polarization potential at higher current densities of 4 mA cm^{-2} and 1 mA cm^{-2}, respectively [Figure 1D and E].

To understand the performance deviation of Zn||Zn symmetric cells in the three hybrid electrolytes, we analyzed the surface evolution of the Zn anodes after 40 h of cycling at 60 °C. Optical images of Zn anodes showed that the surface morphology of Zn anode cycled in G4-based electrolytes was more uniform than those in PC- and DMF-based electrolytes [Insets of Figure 2A-C]. SEM images further revealed significant differences in Zn deposition morphology [Figure 2A-C]. The Zn anode cycled in a G4-based electrolyte displayed dense and uniform deposition [Figure 2A]. In contrast, the Zn anode cycled in PC-based electrolyte was covered with a planar and loose layer, which is ascribed to a solid-electrolyte interphase (SEI) [Figure 2B]. The Zn anode cycled in DMF-based electrolyte showed uneven deposition with pronounced protrusions, associated with the premature cell failure [Figure 2C]. As shown in the EDS mapping in Figure 2D-F, the Zn and F elements were distributed uniformly on the Zn anodes in the

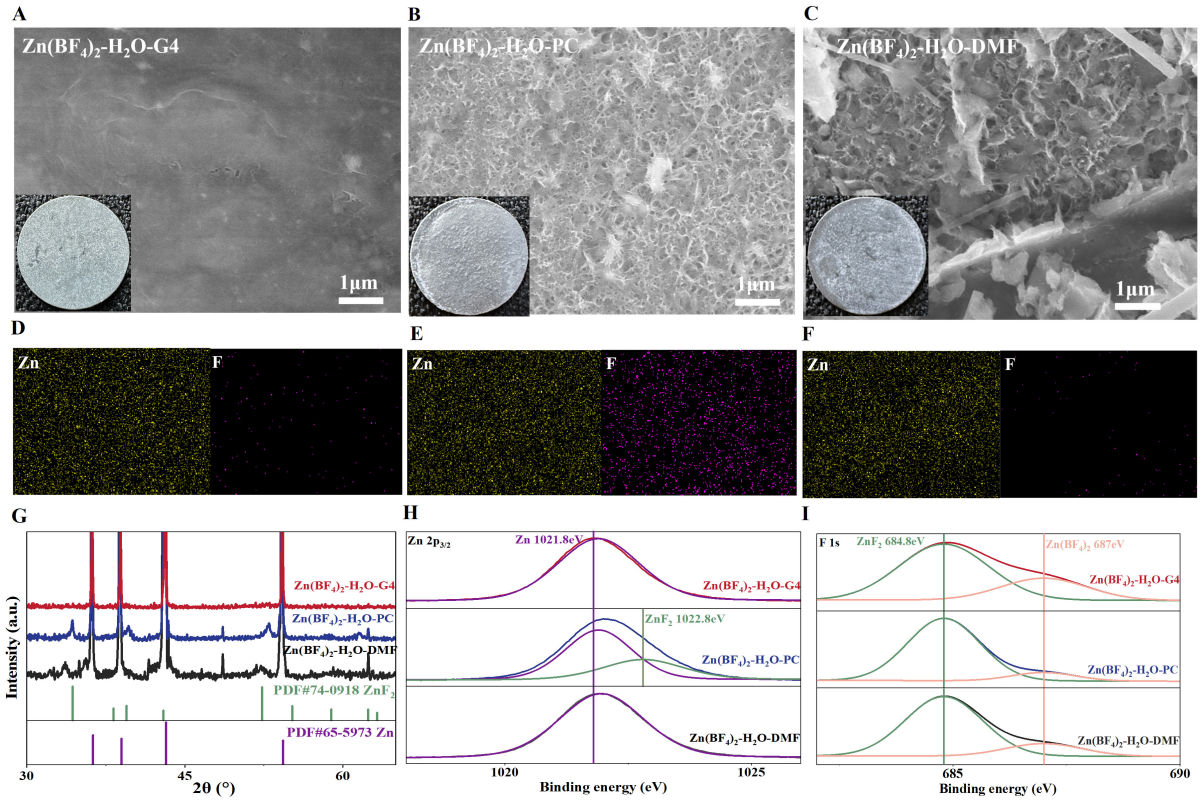

Figure 2. Structure and composition of the Zn anodes after 20 cycles in Zn||Zn symmetric cells. SEM images for the Zn anodes cycled in (A) G4-based; (B) PC-based; and (C) DMF-based hybrid electrolytes; Insets of (A-C) showing the corresponding optical images of the Zn anodes; EDX mapping of Zn and For the Zn anodes cycled in (D) G4-based; (E) PC-based; (F) DMF-based; (G) XRD patterns of Zn anodes cycled in three hybrid electrolytes; XPS spectra of (H) Zn $2p_{3/2}$ and (I) F 1s for Zn anodes cycled in three hybrid electrolytes. PC: Propylene carbonate; DMF: Dimethylformamide; SEM: Scanning electron microscope; XRD: X-ray diffraction; XPS: X-ray photoelectron spectrometer; EDX: Energy dispersive X-ray spectroscopy.

G4- and PC-based electrolytes, while their distribution was nonuniform in the DMF-based electrolyte. Moreover, the amount of F element was evidently larger in PC-based electrolytes than in G4-based and DMF-based electrolytes, due to more ZnF_2 formation in the PC-based electrolyte.

The crystal structure of Zn anodes was analyzed by XRD. As shown in Figure 2G, the characteristic peaks indexed to Zn of the hexagonal crystal were primarily observed in Zn anodes cycled in G4-based and DMF-based electrolytes, suggesting minimal by-product formation. Additional peaks corresponding to ZnF_2 of the tetragonal crystal appeared in the Zn anode cycled in PC-based electrolyte, indicating the formation of ZnF_2 as a component of the SEI. XPS [Supplementary Figure 3] provided interfacial chemistry information, further supporting the above findings. As shown in the Zn $2p_{3/2}$ XPS spectra in Figure 2H, the Zn anode cycled in G4- and DMF-based electrolytes showed higher zinc content. In contrast, the Zn anode cycled in PC-based electrolyte had a greater presence of ZnF_2. The F 1s XPS spectra display characteristic peaks of ZnF_2 and BF_4^- species [Figure 2I], showing that the ZnF_2 proportion was dominant in the PC-based electrolyte, while it was relatively small in the G4-based and DMF-based electrolytes. The larger ZnF_2 content in the PC-based electrolyte is consistent with the EDS mapping. These results suggest that the choice of electrolyte significantly influences the Zn deposition behavior and SEI formation, influencing the electrochemical performance of the cells.

Correlation between Zn^{2+} solvation structure and Zn deposition

To explore the impact of different hybrid electrolytes on the electrochemical performance of Zn||Zn symmetric cells, we conducted detailed characterization and analysis on their physicochemical properties. First, the ionic conductivities of three hybrid electrolytes decreased in the order: DMF-based electrolyte (3.21 mS cm^{-1}) > PC-based electrolyte (2.08 mS cm^{-1}) > G4-based electrolyte (0.56 mS cm^{-1}) [Figure 3A]. The ion transference number followed the same trend [Supplementary Figure 4]: DMF-based electrolyte (0.48) > PC-based electrolyte (0.24) ≈ G4-based electrolyte (0.23). Considering the superior electrochemical performance of G4-based electrolytes despite their lower ionic conductivity and transference number, bulk ion transport is not the decisive factor driving the performance difference. Then, we tested the thermal stability of the electrolytes using an ARC [Figure 3B]. All three electrolytes demonstrated exothermic behavior at temperatures exceeding 150 °C, as confirmed through the ARC. Consequently, thermal stability cannot sufficiently explain the observed performance discrepancy among the hybrid electrolytes. As shown in Figure 3C, the G4-based electrolyte exhibited a more negative stability window when compared with the PC- and DMF-based electrolytes, which is beneficial for alleviated HER.

The interaction between a Zn^{2+} ion and organic solvent(s) was assessed via density functional theory (DFT) calculations. As shown in Figure 3D, the binding energy of Zn^{2+}-G4 (-9.64 eV) was significantly larger than those of Zn^{2+}-PC (-7.71 eV) and Zn^{2+}-DMF (-8.13 eV). The huge binding energy difference (ΔEb > 1.8 eV) indicates a much stronger Zn^{2+}-G4 interaction compared to Zn^{2+}-PC and Zn^{2+}-DMF interactions. From this, we infer that in the solvation structure formed in the G4-based electrolyte, Zn^{2+} ions are primarily coordinated with G4 molecules, with minimal H_2O molecules present. The solvation structure in G4-based electrolyte leads to low conductivity and transference number because of minimal H_2O molecules around Zn^{2+} ions. However, this likely contributes to the suppressed HER and superior performance of the G4-based electrolyte.

To validate the DFT binding energy calculations, we conducted FTIR spectroscopy on the three hybrid electrolytes, and solid $Zn(BF_4)_2{\cdot}xH_2O$ as reference. The O-H stretching vibration of H_2O exhibited a broad band at 3,200-3,600 cm^{-1} [Figure 3E]. An intense peak at around 3,600 cm^{-1} was observed for the solid $Zn(BF_4)_2{\cdot}xH_2O$, attributed to the H_2O molecules strongly coordinated with Zn^{2+} ions. Upon the addition of organic solvents, as for the hybrid electrolytes, the strong peak shifted to lower wavenumbers due to the weakened coordination between H_2O molecules and Zn^{2+} ions. This peak shift was the most pronounced in the G4-based electrolyte, indicating the smallest amount of H_2O molecules in the Zn^{2+} solvation sheath of the G4-based electrolyte. Additionally, for the solid $Zn(BF_4)_2{\cdot}xH_2O$, the characteristic band of the B-F stretching vibration of BF_4^- anions appeared as two peaks at 520-540 cm^{-1} [Figure 3F]. These two distinct peaks were preserved for the PC-based electrolyte despite the peak shifting to higher wavenumbers than the solid $Zn(BF_4)_2{\cdot}xH_2O$, indicating that a certain amount of BF_4^- anions participated in the Zn^{2+} solvation sheath of PC-based electrolyte. Comparatively, the two peaks merged into one for the G4- and DMF-based electrolytes, implying that the BF_4^- anions in Zn^{2+} solvation sheath were replaced by the G4 and DMF solvents. These FTIR results can be explained by the binding energies from DFT calculations. The stronger Zn^{2+}-G4 interaction made the H_2O molecules and BF_4^- anions be excluded from the Zn^{2+} solvation sheath, while the weaker Zn^{2+}-PC interaction made a minor change.

Based on the aforementioned results, the Zn deposition features in the three hybrid electrolytes were correlated with their Zn^{2+} solvation structures. Unlike the previous studies of co-solvent electrolytes, herein, the organic solvents with strong solvation abilities could solve $Zn(BF_4)_2{\cdot}xH_2O$ without extra water[41,42]. In the G4-based electrolyte [Figure 3G], Zn^{2+} ions are predominantly coordinated by G4 molecules, with minor BF_4^- and H_2O in the Zn^{2+} solvation sheath. This, combined with the high thermal stability of the electrolyte, allows for the uniform Zn deposition on the anode and minimized side reactions associated with H_2O. In

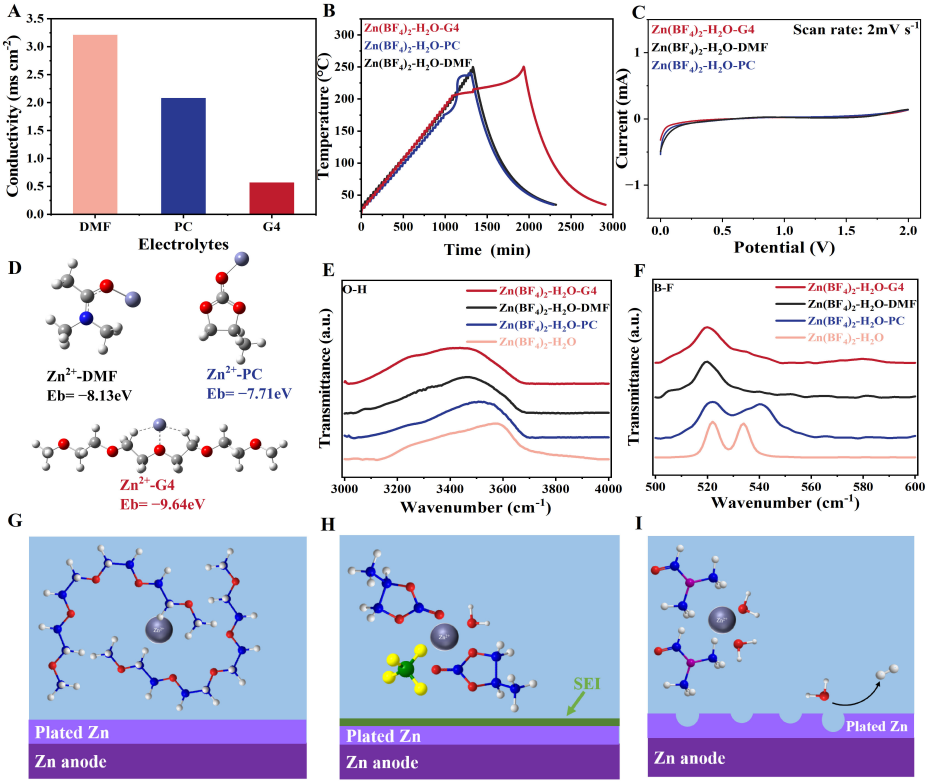

Figure 3. Correlations between electrolyte feature and electrochemical performance of Zn anodes. (A) Ionic conductivity of the three electrolytes; (B) Temperature change *vs.* time during the heatwaitseek mode of three hybrid electrolytes; (C) Electrochemical stability windows of three hybrid electrolytes measured by linear sweep voltammetry curves at a scan rate of 2 mV s^{-1}; (D) The optimized structures and the corresponding binding energies between a Zn^{2+} ion and a solvent(s) from DFT calculations; FTIR spectra showing (E) the O-H stretching vibration of H_2O and (F) the B-F stretching vibration of BF_4^- for three hybrid electrolytes; Schematics showing the Zn deposition behaviors on the Zn anode in (G) G4-based; (H) PC-based; and (I) DMFbased hybrid electrolytes. Color mapping: Zn gray, C blue, O red, H white, B green, F yellow, N purple. DFT: Density functional theory; FTIR: Fourier transform infrared; PC: Propylene carbonate; DMF: Dimethylformamide.

contrast, in the PC-based electrolyte [Figure 3H], both BF_4^- and H_2O are coordinated with Zn^{2+} ions. The involvement of BF_4^- in the Zn^{2+} solvation sheath contributes to the formation of protective ZnF_2-based SEI on the Zn anode. In contrast, the presence of H_2O in the Zn^{2+} solvation sheath promotes H_2O-associated side reactions at high temperatures, which, over time, degrades the cell performance. In the DMF-based electrolyte [Figure 3I], a large amount of H_2O participates in the Zn^{2+} solvation sheath without the presence of BF_4^-, causing severe side reactions and thus the poorest performance among the three electrolytes. Compared with the PC- and DMF-based electrolytes, the G4-based electrolyte exhibited a more stable Zn^{2+} solvation sheath with considerably lower water content, leading to its superior high-temperature performance.

Full cells based on various hybrid electrolytes

The practical application of the hybrid electrolytes was further demonstrated by assembling full cells using Zn as the anode and AC as the cathode[43], and the electrochemical tests were conducted at 60 °C. Figure 4A-C shows the CV curves of the three Zn||AC full cells at different scan rates, presenting nearly regular shapes in the range from 0.1 to 1.6 V attributed to the capacitive behavior of the AC electrode. To examine the rate performance of three Zn||AC full cells, GCD curves at various current densities were measured [Supplementary Figure 5]. It can be found that G4-based electrolyte exhibits a lower rate

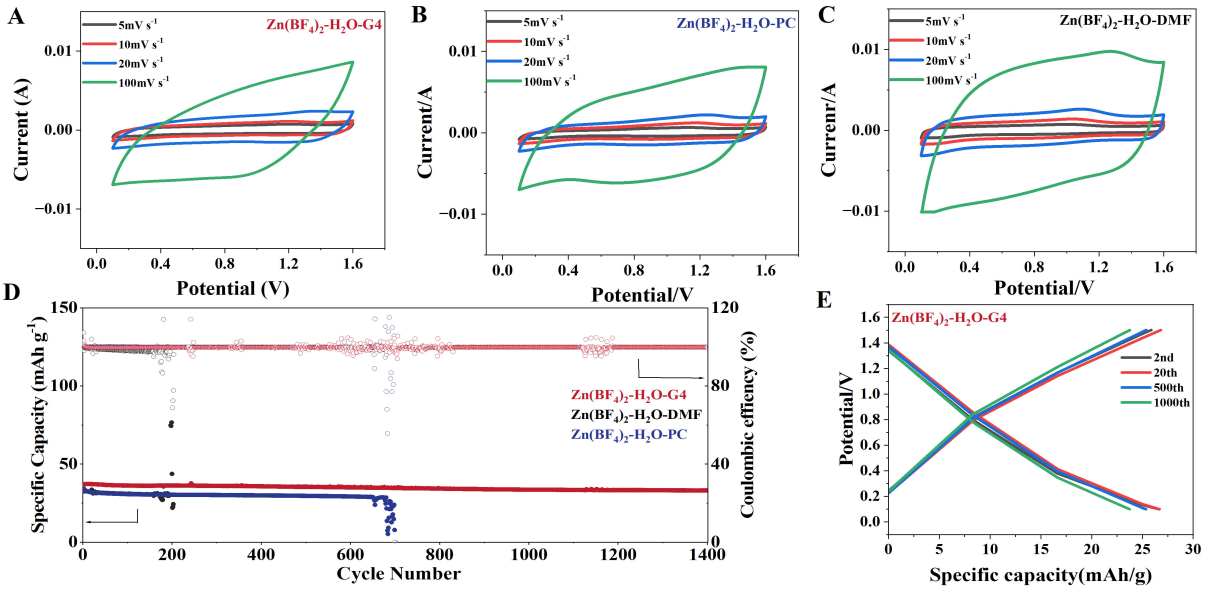

Figure 4. Electrochemical performances of Zn||AC full cells. CV curves at various scan rates using (A) G4-based; (B) PCbased; and (C) DMFbased hybrid electrolytes; (D) Cycling stability at 0.5A g^{-1} for the full cells using three hybrid electrolytes; (E) GCD curves of the full cell using G4-based-electrolyte at 0.5 A g^{-1} from the 2nd to 1,000th cycle at 60 °C. PC: Propylene carbonate; DMF: Dimethylformamide; CV: Cyclic voltammetry; GCD: Galvanostatic charge/discharge.

capability (retained 63% capacitance from 0.2 to 2A g^{-1}) than those of DMF-based (77%) and PC-based (75%) electrolytes, which was explained by the low conductivity of G4-based electrolyte. The GCD tests were further conducted at a current density of 0.5 A g^{-1} to evaluate the cycling stability of the Zn||AC full cells. As summarized in Figure 4D, the cell using G4-based electrolyte demonstrated superior cycling stability, showing 90.7% capacity retention after 1,400 cycles. The GCD curves maintained their linear shape without evident deformation over the long cycling test, highlighting the stability of the G4-based electrolyte [Figure 4E]. In contrast, the PC-based hybrid electrolyte exhibited a sharp capacity decline after ~650 cycles, accompanied by noticeable fluctuations in coulombic efficiency [Figure 4D and Supplementary Figure 6A]. The cell using DMF-based electrolyte showed a marked drop in capacity after just ~150 cycles [Figure 4D and Supplementary Figure 6B], which should be attributed to the Zn dendrite growth and side reactions. Therefore, the G4-based hybrid electrolyte also improved the cycling stability of full cells.

CONCLUSION

In conclusion, we designed hybrid electrolytes consisting of $Zn(BF_4)_2{\cdot}xH_2O$ and different organic solvents (PC, DMF, G4) for high-temperature ZIBs. As elaborated via theoretical simulations and spectroscopic characterizations, the more reversible and uniform Zn deposition at 60 °C in the G4-based electrolyte was attributed to the strong Zn^{2+}-G4 interaction and the unique Zn^{2+} solvation structure primarily surrounded by G4 molecules, which significantly suppressed H_2O associated side reactions. The superiority of the G4-based electrolyte was further confirmed by assembling a zinc-ion capacitor full cell, which maintained stable performance for > 1,400 cycles at 60 °C, outperforming the other two hybrid electrolytes. This study provides molecular insights into the design of Zn^{2+} solvation structure for Zn anodes and would drive further electrolyte exploration for high-temperature energy storage technologies. However, the low ionic conductivity of G4-based electrolytes and short cycling life at more enhanced temperatures are not addressed. Future research directions would be utilizing electrolyte additives or organic co-solvents to improve the overall performance of the hybrid electrolytes for ZIBs.

DECLARATIONS

Authors' contributions

Research design, manuscript drafting: Xie, Y.
Material characterization, formal analysis: Xie, Y.; Li, G.; Chen, Y.
Review, supervision, manuscript drafting, funding acquisition: Dou, Q.; Yan, X.

Availability of data and materials

The data is accessible and available upon request from the authors.

Financial support and sponsorship

This work was supported by the National Natural Science Foundation of China (22279166, 22309211); the Guangdong Basic and Applied Basic Research Foundation (2022B1515120019, 2024A1515010158); the Young Talent Support Project of Guangzhou Association for Science and Technology; the Fundamental Research Funds for the Central Universities, Sun Yat-sen University (22qntd0101, 23qnpy02).

Conflicts of interest

All authors declared that there are no conflicts of interest.

Ethical approval and consent to participate

Not applicable.

Consent for publication

Not applicable.

REFERENCES

1. Li, Z.; Tan, J.; Wang, Y.; et al. Building better aqueous Zn-organic batteries. *Energy. Environ. Sci.* **2023**, *16*, 2398-431. DOI
2. Wang, Y.; Li, Q.; Hong, H.; et al. Lean-water hydrogel electrolyte for zinc ion batteries. *Nat. Commun.* **2023**, *14*, 3890. DOI PubMed PMC
3. Gourley, S. W.; Brown, R.; Adams, B. D.; Higgins, D. Zinc-ion batteries for stationary energy storage. *Joule* **2023**, *7*, 1415-36. DOI
4. Cao, J.; Zhang, D.; Chanajaree, R.; et al. A low-cost separator enables a highly stable zinc anode by accelerating the de-solvation effect. *Chem. Eng. J.* **2024**, *480*, 147980. DOI
5. Zong, Y.; He, H.; Wang, Y.; et al. Functionalized separator strategies toward advanced aqueous zinc-ion batteries. *Adv. Energy. Mater.* **2023**, *13*, 2300403. DOI
6. Chen, J.; Zhao, W.; Jiang, J.; et al. Challenges and perspectives of hydrogen evolution-free aqueous Zn-ion batteries. *Energy. Storage. Mater.* **2023**, *59*, 102767. DOI
7. Fang, G.; Zhou, J.; Pan, A.; et al. Recent advances in aqueous zinc-ion batteries. *ACS. Energy. Lett.* **2018**, *3*, 2480-501. DOI
8. Heptonstall, P. J.; Gross, R. J. K. A systematic review of the costs and impacts of integrating variable renewables into power grids. *Nat. Energy.* **2021**, *6*, 72-83. DOI
9. Chen, M.; Chen, J.; Zhou, W.; Han, X.; Yao, Y.; Wong, C. P. Realizing an all-round hydrogel electrolyte toward environmentally adaptive dendrite-free aqueous Zn-MnO_2 batteries. *Adv. Mater.* **2021**, *33*, e2007559. DOI
10. Xiao, D.; Lv, X.; Fan, J.; Li, Q.; Chen, Z. Zn-based batteries for energy storage. *Energy. Mater.* **2023**, *3*, 300007. DOI
11. Liu, Z.; Cui, T.; Pulletikurthi, G.; et al. Dendrite-free nanocrystalline zinc electrodeposition from an ionic liquid containing nickel triflate for rechargeable Zn-based batteries. *Angew. Chem. Int. Ed.* **2016**, *55*, 2889-93. DOI
12. Yin, Y.; Li, X. Review and perspectives on anodes in rechargeable aqueous zinc-based batteries. *Renewables* **2023**, *1*, 622-37. DOI
13. Wang, S.; Yuan, C.; Chang, N.; et al. Act in contravention: a non-planar coupled electrode design utilizing "tip effect" for ultra-high areal capacity, long cycle life zinc-based batteries. *Sci. Bull.* **2021**, *66*, 889-96. DOI
14. Cao, Q.; Pan, Z.; Gao, Y.; et al. Stable imprinted zincophilic Zn anodes with high capacity. *Adv. Funct. Mater.* **2022**, *32*, 2205771. DOI
15. Xu, C.; Li, B.; Du, H.; Kang, F. Energetic zinc ion chemistry: the rechargeable zinc ion battery. *Angew. Chem. Int. Ed.* **2012**, *51*, 933-5. DOI

16. Li, H.; Ma, L.; Han, C.; et al. Advanced rechargeable zinc-based batteries: recent progress and future perspectives. *Nano. Energy.* **2019**, *62*, 550-87. DOI
17. Fu, J.; Cano, Z. P.; Park, M. G.; Yu, A.; Fowler, M.; Chen, Z. Electrically rechargeable zinc-air batteries: progress, challenges, and perspectives. *Adv. Mater.* **2017**, 29. DOI PubMed
18. Wu, B.; Wu, Y.; Lu, Z.; et al. A cation selective separator induced cathode protective layer and regulated zinc deposition for zinc ion batteries. *J. Mater. Chem. A.* **2021**, *9*, 4734-43. DOI
19. Zeng, X.; Zhang, S.; Long, T.; et al. An amphipathic ionic sieve membrane for durable and dendrite-free zinc-ion batteries. *Renewables* **2024**, *2*, 52-60. DOI
20. Hu, L.; Xiao, P.; Xue, L.; Li, H.; Zhai, T. The rising zinc anodes for high-energy aqueous batteries. *EnergyChem* **2021**, *3*, 100052. DOI
21. Lu, K.; Zhang, H.; Song, B.; Pan, W.; Ma, H.; Zhang, J. Sulfur and nitrogen enriched graphene foam scaffolds for aqueous rechargeable zinc-iodine battery. *Electrochim. Acta.* **2019**, *296*, 755-61. DOI
22. Zhang, Y.; Bi, S.; Niu, Z.; Zhou, W.; Xie, S. Design of Zn anode protection materials for mild aqueous Zn-ion batteries. *Energy. Mater.* **2022**, *2*, 200012. DOI
23. Zhang, X.; Weng, H.; Miu, Y.; et al. Atomic-scale inorganic carbon additive with rich surface polarity and low lattice mismatch for zinc to boost Zn metal anode reversibility. *Chem. Eng. J.* **2024**, *482*, 148807. DOI
24. Yang, J.; Yin, B.; Sun, Y.; et al. Zinc anode for mild aqueous zinc-ion batteries: challenges, strategies, and perspectives. *Nano-Micro. Lett.* **2022**, *14*, 42. DOI PubMed PMC
25. Nian, Q.; Wang, J.; Liu, S.; et al. Aqueous batteries operated at -50 °C. *Angew. Chem. Int. Ed.* **2019**, *58*, 16994-9. DOI
26. Chen, T. Y.; Lin, T. J.; Vedhanarayanan, B.; Shen, H. H.; Lin, T. W. Optimization of acetamide based deep eutectic solvents with dual cations for high performance and low temperature-tolerant aqueous zinc ion batteries via tuning the ratio of co-solvents. *J. Colloid. Interface. Sci.* **2023**, *629*, 166-78. DOI PubMed
27. Shi, Y.; Wang, R.; Bi, S.; Yang, M.; Liu, L.; Niu, Z. An anti-freezing hydrogel electrolyte for flexible zinc-ion batteries operating at -70 °C. *Adv. Funct. Mater.* **2023**, *33*, 2214546. DOI
28. Samanta, P.; Ghosh, S.; Kundu, A.; Samanta, P.; Murmu, N. C.; Kuila, T. Recent progress on the performance of Zn-ion battery using various electrolyte salt and solvent concentrations. *ACS. Appl. Electron. Mater.* **2023**, *5*, 100-16. DOI
29. Yang, F.; Yuwono, J. A.; Hao, J.; et al. Understanding H_2 evolution electrochemistry to minimize solvated water impact on zinc-anode performance. *Adv. Mater.* **2022**, *34*, e2206754. DOI
30. Liu, C.; Xie, X.; Lu, B.; Zhou, J.; Liang, S. Electrolyte strategies toward better zinc-ion batteries. *ACS. Energy. Lett.* **2021**, *6*, 1015-33. DOI
31. Du, Y.; Li, Y.; Xu, B. B.; et al. Electrolyte salts and additives regulation enables high performance aqueous zinc ion batteries: a mini review. *Small* **2022**, *18*, e2104640. DOI
32. Jin, Y.; Han, K. S.; Shao, Y.; et al. Stabilizing zinc anode reactions by polyethylene oxide polymer in mild aqueous electrolytes. *Adv. Funct. Mater.* **2020**, *30*, 2003932. DOI
33. Sun, T.; Zheng, S.; Du, H.; Tao, Z. Synergistic effect of cation and anion for low-temperature aqueous zinc-ion battery. *Nanomicro. Lett.* **2021**, *13*, 204. DOI PubMed PMC
34. Zhang, N.; Dong, Y.; Jia, M.; et al. Rechargeable aqueous Zn-V_2O_5 battery with high energy density and long cycle life. *ACS. Energy. Lett.* **2018**, *3*, 1366-72. DOI
35. Wang, N.; Yang, Y.; Qiu, X.; Dong, X.; Wang, Y.; Xia, Y. Stabilized rechargeable aqueous zinc batteries using ethylene glycol as water blocker. *ChemSusChem* **2020**, *13*, 5556-64. DOI
36. Liu, S.; Zhang, R.; Mao, J.; Zhao, Y.; Cai, Q.; Guo, Z. From room temperature to harsh temperature applications: Fundamentals and perspectives on electrolytes in zinc metal batteries. *Sci. Adv.* **2022**, *8*, eabn5097. DOI PubMed PMC
37. Zhang, Q.; Xu, S.; Wang, Y.; Dou, Q.; Sun, Y.; Yan, X. Temperature-dependent structure and performance evolution of "water-in-salt" electrolyte for supercapacitor. *Energy. Storage. Mater.* **2023**, *55*, 205-13. DOI
38. Li, X.; Ji, C.; Shen, J.; et al. Amorphous heterostructure derived from divalent manganese borate for ultrastable and ultrafast aqueous zinc ion storage. *Adv. Sci.* **2023**, *10*, e2205794. DOI PubMed PMC
39. Ma, L.; Chen, S.; Li, N.; et al. Hydrogen-free and dendrite-free all-solid-state Zn-ion batteries. *Adv. Mater.* **2020**, *32*, e1908121. DOI
40. Edmondson, G. K.; Benisek, L. 27-solvent-applied flame-resist treatments for wool, cotton, and wool-cotton blends. *J. Text. Inst.* **1977**, *68*, 230-9. DOI
41. Kao-Ian, W.; Sangsawang, J.; Gopalakrishnan, M.; et al. Preinserted ammonium in MnO_2 to enhance charge storage in dimethyl sulfoxide based zinc-ion batteries. *ACS. Appl. Mater. Interfaces.* **2024**, *16*, 56926-34. DOI
42. Wang, Z.; Bai, L.; Fan, H.; Wang, Y.; Liu, W. Solvation strategies in various electrolytes for advanced zinc metal anode. *J. Energy. Chem.* **2024**, *94*, 740-57. DOI
43. Sun, Y.; Ma, H.; Zhang, X.; et al. Salty ice electrolyte with superior ionic conductivity towards low-temperature aqueous zinc ion hybrid capacitors. *Adv. Funct. Mater.* **2021**, *31*, 2101277. DOI